ITU-R P.618/P.838 Rain-Attenuation Extension of 3GPP TR 38.811 Aligned GEO NTN-TDL Channel Model in OpenAirInterface5G

Sumit Kumar*, Ion Turcanu*
*Luxembourg Institute of Science and Technology
{sumit.kumar, ion.turcanu}@list.lu

Abstract*—5G-NTN extends cellular connectivity through satellite systems, but realistic evaluation of such networks requires channel models that capture the distinct propagation characteristics of Earth-space links. Existing open-source end-to-end 5G NTN experimentation platforms provide limited support for standardized NTN channel models that jointly represent small-scale fading, elevation-dependent large-scale effects, LOS/NLOS conditions, and weather-dependent attenuation. This paper addresses this gap by developing a 3GPP TR 38.811-aligned GEO NTN tapped-delay-line channel model within the OpenAirInterface5G (OAI), supporting NTN-TDL-A/B/C/D profiles, LOS/NLOS-aware profile remapping, and elevation-dependent large-scale propagation effects. The model is further extended with ITU-R P.618/P.838 rain attenuation to capture frequency-, elevation-, and rain-rate-dependent rain loss. The implementation is validated through consistency checks, downlink and uplink BLER sweeps over S-, Ku-, and Ka-band frequencies and multiple elevation angles, and end-to-end OAI gNB/UE 5G SA attach experiments. Results show negligible rain impact at S-band, substantial degradation at Ku-band, and severe Ka-band impairment under heavy rain, with higher elevation angles consistently reducing the rain-induced loss. End-to-end RFsim experiments further confirm successful 5G SA attachment while preserving the expected LOS/NLOS channel-profile behavior under the tested rain conditions. The resulting implementation provides a reproducible, standards-aligned channel- and PHY-level environment for studying realistic GEO 5G-NTN propagation effects within OAI. The channel-model extensions are being prepared for integration into the OAI develop branch, with the aim of making them available to the broader OAI NTN community.

I. Introduction

Fifth-generation Non-Terrestrial Networks (5G-NTN) extend cellular connectivity beyond terrestrial coverage through satellite systems operating in geostationary (GSO) and non-geostationary (NGSO) orbits. The substantially different propagation conditions of satellite links, including long propagation delays, Doppler shifts, and elevation-dependent channel characteristics, require channel models specifically tailored to 5G-NTN operation. To support such studies, 3GPP TR 38.811 [1] defines representative NTN channel models, including tapped-delay-line (TDL) small-scale fading profiles and large-scale effects such as free-space path loss, clutter loss, and LOS/NLOS conditions.

For GEO satellite links, atmospheric propagation effects can introduce additional impairments beyond those represented by the TR 38.811 channel models. In particular, rain attenuation can become significant at higher carrier frequencies and varies strongly with carrier frequency, elevation angle, and rain rate. ITU-R Recommendations P.618 [2] and P.838 [3] provide established methods for characterizing this attenuation for Earth-space links. Therefore, studying rain effects together with standardized 5G-NTN channel conditions requires a TR 38.811-consistent GEO NTN-TDL model augmented with an explicit ITU-R rain-attenuation component.

OpenAirInterface5G (OAI) [4] is a prominent open-source platform for 5G and beyond experimentation and provides a practical environment for prototyping and evaluating NTN functionalities. Its RF simulator (RFsim) currently supports a limited set of satellite-relevant propagation effects in a single-path setting, including propagation delay and Doppler. However, GEO RFsim does not provide a composite TR 38.811-aligned channel model combining NTN-TDL multipath profiles, elevation-dependent large-scale effects, and LOS/NLOS-aware channel conditions. In this work, we first establish such a GEO NTN-TDL channel model in OAI RFsim and then extend it with ITU-R P.618/P.838 rain attenuation. The proposed extension incorporates ITU-R P.618/P.838 rain attenuation, using P.838 specific-attenuation coefficients within the P.618 Earth-space path calculation, enabling controlled rain-sensitivity studies without modifying the underlying TR 38.811 tap structure.

The main contributions are as follows:

- *TR 38.811-aligned GEO NTN-TDL baseline for OAI RFsim:* we extend OAI RFsim with a GEO channel substrate combining `NTN_TDL_A/B/C/D` small-scale profiles, elevation-dependent large-scale loss, and LOS/NLOS-aware profile remapping. This fills a gap left by existing OAI NTN simulator, which currently applies only a fixed propagation delay without a composite TR 38.811 channel model.
- *ITU-R P.618/P.838 rain-attenuation integration:* we add an ITU-R P.618 $A_{0.01}$ rain-attenuation term to the GEO channel path using ITU-R P.838 specific attenuation coefficients, with configurable $R_{0.01}$, carrier frequency, elevation, rain height, station altitude, latitude, and polarization tilt, applied as a large-scale loss term independent of the TR 38.811 tap structure.

© 2026 IEEE. Personal use of this material is permitted. Permission from IEEE must be obtained for all other uses, in any current or future media, including reprinting/republishing this material for advertising or promotional purposes, creating new collective works, for resale or redistribution to servers or lists, or reuse of any copyrighted component of this work in other works.

IEEE International Conference on Advanced Networks and Telecommunications Systems (ANTS 2026)

- *Reproducible DL/UL PHY sensitivity evaluation:* we validate the extension through deterministic sanity checks, downlink/uplink BLER sweeps across NTN-TDL-A/B/C/D, S/Ku/Ka carrier bands, 30°/60° elevation, and clear/moderate/heavy rain scenarios, quantifying the SNR cost of rain at each band and outage regimes.
- *End-to-end RFsim validation under rain:* we evaluate the proposed channel model using paired OAI gNB/UE RFsim softmodems under GEO LOS/NLOS and rain conditions. The experiments confirm successful end-to-end 5G SA attachment while preserving the expected LOS/NLOS-aware NTN-TDL profile remapping under rain adjusted channel conditions.

II. Related Work

At the link level, the MathWorks Satellite Communications Toolbox exposes TR 38.811 NTN-TDL parameters through objects such as `nrTDLChannel`, enabling inspection of tap delays, average path gains, and Ricean K-factors [5]. It serves as a useful reference for verifying TR 38.811 tap parameters but not designed for end-to-end 5G system simulation over a full protocol stack. OpenNTN [6] extends Sionna with TR 38.811 cluster-ray channel generation, including large-scale loss, LOS/NLOS, and satellite/UT antenna patterns; however, it does not provide the link-level NTN-TDL A/B/C/D profiles of TR 38.811, so standardized tap-delay-line tables cannot be instantiated.

At the system-simulation level, Sandri *et al.* [7] integrated TR 38.811 NTN channel elements into ns-3, including geocentric mobility, elevation-dependent path loss, clutter, shadow fading, and scintillation. Their small-scale fading uses NTN-CDL models with elevation-dependent statistics, rather than the standard NTN-TDL-A/B/C/D link-level profiles (in contrast to MathWorks `nrTDLChannel` implementation). Besides, SNS3 [8] provides a ns-3 satellite extension focused on constellation topology, MAC/scheduling, and packet-level performance across LEO, MEO, and GEO orbits, rather than on validating NR PHY/stack attach over TR 38.811 NTN-TDL channel profiles.

Furthermore, at the system level, srsRAN Project [9], [10] supports Release-17 NTN gNB configuration, including SIB19, extended RRC/MAC timers, and GEO timing parameters, and shows end-to-end attach, however, its publicly documented channel emulator applies only a fixed propagation delay and does not implement TR 38.811 NTN-TDL channel model, that is, elevation-dependent large-scale loss, clutter, shadow fading, or LOS/NLOS-consistent tap selection. srsRAN therefore addresses NTN protocol timing and connectivity rather than standardized satellite channel modeling.

OAI [4] has been successfully used for 5G-NTN experimentations over emulated and live satellite links, with Release-17 NTN adaptations summarized in [11], GEO demonstrators reported in [12]–[14], and an LEO-based demonstrator in [15]. These efforts established protocol-stack timing, synchronization, and end-to-end connectivity, but currently GEO RFsim setups in OAI use fixed delay only and do not expose composite models that combine NTN-TDL taps with elevation-dependent loss and LOS/NLOS profiles from TR 38.811.

Taken together, no existing OAI-based or third-party framework combines standardized TR 38.811 NTN-TDL small-scale profiles, elevation-dependent LOS/NLOS-aware large-scale loss, and an ITU-R P.618/P.838 rain-attenuation term within a single, PHY- and attach-validated GEO channel model. This paper addresses that gap directly within OAI.

TABLE I
GEO NTN-TDL BASELINE

Element	Description
NTN-TDL profiles	TR 38.811 Sec. 6.9.2 `NTN_TDL_A/B/C/D` tap profiles providing small scale fading
GEO composites in OAI	`SAT_GEO_NTN_TDL_A/B/C/D` expose the profiles on the RFsim `chanmod` path.
Large-scale terms	Elevation-dependent relative FSPL, clutter, and reciprocal shadow fading provide the GEO large-scale state before rain is added.
Link-state handling	Configured LOS/NLOS state selects the effective tap family through initialization-time A/C and B/D remapping.
RFsim timing	GEO propagation delay remains on `rfsimulator.prop_delay`; NTN-TDL taps represent excess multipath around the UE.

TABLE II
BASELINE SANITY CHECKS BEFORE ADDING RAIN ATTENUATION

Validation Check	Outcome
Static descriptors	Tap delays, normalized powers, and Ricean K-factors for A/B/C/D match TR 38.811 Sec. 6.9.2 tables.
PHY behavior	DL/UL unitary sweeps preserve expected A/B versus C/D behavior; an independent MathWorks 5G Toolbox comparison confirmed the dominant sample-bin power structure.
GEO resolver	LOS probability, shadowing spread, delay-spread, relative FSPL, and profile remapping checks follow the encoded TR 38.811 rules.
RFsim attach logs	Configured 30°/60° urban LOS/NLOS runs completed the expected 5G SA attach-log sequence.

III. ITU-R P.618/P.838 Rain-Attenuation Extension

A. GEO NTN-TDL Baseline

For the ITU-R P.838 rain-attenuation extension, we first establish a GEO NTN-TDL baseline in OAI RFsim incorporating the TR 38.811 small-scale fading profiles, LOS/NLOS remapping, elevation-dependent free-space path loss, clutter loss, and shadow fading, as summarized in Table I. Building on this baseline, we incorporate an additional rain-induced attenuation component based on the ITU-R P.838 specific rain attenuation model.

B. Rain-Attenuation Model and Integration

The extension follows the separation between the 3GPP NTN channel model and ITU-R Earth-space rain-propagation effects. TR 38.811 remains the basis for the GEO NTN-TDL tap profiles and large-scale LOS/NLOS channel conditions. Rain attenuation is incorporated using the ITU-R P.618 Earth-space

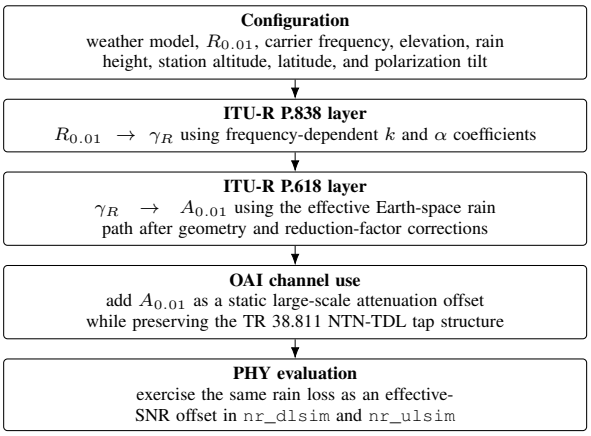


Fig. 1. Rain-attenuation implementation flow. The rain-attenuation model remains separate from the TR 38.811 small-scale channel: NTN-TDL tap parameters are unchanged, while ITU-R P.618/P.838 rain attenuation is applied only to the large-scale link loss.

prediction procedure [2], with the specific rain attenuation derived from the ITU-R P.838 coefficients k and α [3]. Specifically, the implementation first computes

$$\gamma_R = kR_{0.01}^{\alpha}, \tag{1}$$

where γ_R is the specific rain attenuation in dB/km and $R_{0.01}$ denotes the rain rate exceeded for 0.01% of an average year, expressed in mm/h. In the present implementation, $R_{0.01}$ is provided as a user-configurable static input rather than being derived from ITU-R P.837/P.839 climatic maps or modeled as a time-varying rain trace. The ITU-R P.618 procedure then converts γ_R into the corresponding Earth-space rain attenuation $A_{0.01}$ by accounting for the link geometry and effective rain-path length. In compact form,

$$A_{0.01} = \gamma_R L_{\text{eff}}, \tag{2}$$

where L_{eff} denotes the effective rain-path length after applying the P.618 geometrical and path-reduction corrections.

The calculation uses the carrier frequency, elevation angle, station latitude and altitude, rain height h_R, and polarization tilt angle τ to determine the effective rain-path geometry and associated reduction factors. Accordingly, $A_{0.01}$ represents the rain attenuation exceeded for 0.01% of an average year for the configured Earth-space link conditions. The resulting rain attenuation is then incorporated as an additional large-scale loss component in the GEO link budget:

$$L_{\text{GEO}} = L_{\text{base}} + \Delta L_{\text{FSPL}} + L_{\text{clutter}} + L_{\text{shadow}} + A_{0.01}. \tag{3}$$

Since $A_{0.01}$ is computed once per scenario as a static large-scale offset, the rain-attenuation extension adds negligible overhead to the RFsim channel path.

Fig. 1 summarizes the implementation flow to PHY-level evaluation.

IV. Validation and Results

A. GEO Rain-Attenuation Model Validation

For reproducibility, the validation uses three default rain settings: clear sky ($R_{0.01} = 0$), moderate rain ($R_{0.01} = 10$ mm/h), and heavy rain ($R_{0.01} = 50$ mm/h), with a default reference geometry of latitude 0°, station altitude 0 km, rain height 5 km, and polarization tilt 45°. A dedicated validator performs deterministic rain-attenuation validation together with the existing GEO free-space path-loss and NTN-TDL remapping checks. It checks four expected properties: (a) zero $R_{0.01}$ produces zero additional loss, (b) increasing $R_{0.01}$ increases attenuation, (c) lower elevation increases rain loss through the longer effective Earth-space path, and (d) Ka-band rain attenuation is much larger than S-band attenuation under the same $R_{0.01}$. The resulting added rain attenuation is summarized in the full PHY-sweep matrix in Table IV, which reports the P.618/P.838 computation across all tested bands and elevations.

B. Downlink BLER Sensitivity to Rain Attenuation

To quantify the PHY-level impact of the rain-attenuation extension, we ran `nr_dlsim` in OAI for BLER sweeps using the simulation parameters in Table III. With 1000 trials per SNR point, BLER estimates below approximately 10^{-2} carry increasing statistical uncertainty; the reported thresholds should be read as indicative of the waterfall region rather than precise outage points. Table IV isolates the additional rain attenuation applied by the rain model across carrier frequency, elevation, and $R_{0.01}$, using a fixed rain geometry so that these three factors can be studied independently. Fig. 2 visualizes the same rain-loss values and highlights the band and elevation dependence of the ITU-R P.618/P.838 attenuation term. The results show that the added loss is negligible at S-band, becomes significant at Ku-band, and becomes severe at Ka-band under heavy rain; higher elevation consistently reduces the added loss, since it shortens the effective Earth-space rain path.

Beyond isolating these factors, we also check whether the P.618 geometry inputs themselves; rather than just frequency, elevation, and rain rate; meaningfully affect the computed attenuation, and whether any such change is large enough to shift the BLER threshold. Table V reports this targeted geometry check: the heavy-rain rows use the main -4–24 dB SNR grid, while the moderate-rain rows use a 0.5 dB fine grid from 17 to 21 dB around the BLER threshold. The second geometry (latitude 49.6°, station altitude 0.3 km) is representative of a mid-latitude ground-station deployment, distinct from the equatorial default reference geometry used elsewhere in the sweeps.

Fig. 3 shows a selected `NTN_TDL_C` sweep. Clear-sky curves have comparable transition regions across all three bands, since the same PHY configuration is used; the separation between curves is therefore due to added rain attenuation. At 2.5 GHz, added loss stays below 0.1 dB even at 50 mm/h. At 14 GHz, 10 mm/h shifts the curve by about 5.8 dB at 30°,

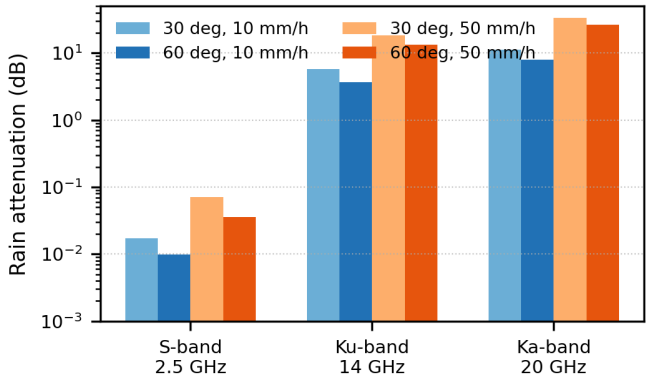


Fig. 2. Added ITU-R P.618 $A_{0.01}$ rain attenuation versus carrier band, elevation, and configured $R_{0.01}$ on a log-scale dB axis. The plot visualizes the same rain-loss values summarized in Table IV: S-band loss remains negligible, while Ku- and Ka-band losses grow sharply under heavier rain and lower elevation.

TABLE III
SIMULATION PARAMETERS FOR THE RAIN-ATTENUATION PHY SWEEPS

Parameter	Value
Simulators	`nr_dlsim` for downlink and `nr_ulsim` for uplink
Channel profiles	`NTN_TDL_A/B/C/D`
Carrier bands	S/Ku/Ka: 2.5/14/20 GHz
Elevation angles	30° and 60°
Rain scenarios	`clear_sky`: $R_{0.01} = 0$ mm/h; `moderate_rain`: $R_{0.01} = 10$ mm/h; `heavy_rain`: $R_{0.01} = 50$ mm/h
Rain model inputs	latitude 0°, station altitude 0 km, rain height 5 km, polarization tilt 45°
Rain-loss application	$A_{0.01}$ applied as an effective SNR offset while keeping the NTN-TDL tap profile unchanged
PHY configuration	DL: 25 PRB, MCS 0; UL: 25 PRB carrier, 25 PRB scheduled PUSCH, numerology 0, MCS 0
SNR grid	-4 to 24 dB in 2 dB steps
Trials	1000 per SNR point

while 50 mm/h pushes the low-BLER region much higher. At 20 GHz, 50 mm/h adds about 33.8 dB at 30°, keeping DL BLER close to outage over the tested SNR range.

This monotonic S-to-Ku-to-Ka increase in rain sensitivity follows directly from the frequency-dependent P.838 coefficients in the P.618 calculation. S-band rain is a small perturbation with no visible effect on the BLER waterfall; Ku-band attenuation is a meaningful link-margin penalty, costing several additional dB of SNR for the same BLER; Ka-band rain can dominate the link budget under heavy rain, making recovery infeasible within a moderate SNR grid. Elevation offers partial mitigation: 60° shortens the rain path and lowers attenuation relative to 30°, but not enough to recover the heavy rain Ka band case.

Finally, Table VI summarizes the Ka band result across all four NTN-TDL profiles, using the first requested SNR where DL BLER falls below 0.1. The absolute threshold depends on the small-scale profile, but the rain trend is consistent: moderate rain shifts the required SNR upward, and heavy rain is not recovered within the tested 24 dB grid. 60° cases have lower P.618 attenuation than 30°, but the 50 mm/h penalty still exceeds the tested grid. The NR entries in Table VI

TABLE IV
ADDED ITU-R P.618 $A_{0.01}$ RAIN ATTENUATION USED IN THE 1000-TRIAL PHY SWEEPS

Band	30°, 10	60°, 10	30°, 50	60°, 50
S, 2.5 GHz	0.017	0.010	0.070	0.036
Ku, 14 GHz	5.766	3.661	18.547	13.460
Ka, 20 GHz	11.283	7.890	33.825	26.519

TABLE V
TARGETED DL GEOMETRY CONFIGURABILITY CHECK FOR `NTN_TDL_C` AT KA-BAND AND 30° ELEVATION. THE 10 MM/H THRESHOLDS USE A 0.5 DB FINE GRID FROM 17 TO 21 DB; NR MEANS NOT REACHED IN THE MAIN -4–24 DB GRID FOR THE 50 MM/H ROWS

Geometry	$R_{0.01}$	$A_{0.01}$	BLER ≤ 0.1
Default: 0°, 0 km, $h_R = 5$ km, $\tau = 45°$	10 mm/h	11.283 dB	19.5 dB
Luxembourg-like: 49.6°, 0.3 km, $h_R = 5.2$ km, $\tau = 0°$	10 mm/h	10.504 dB	19.5 dB
Default: 0°, 0 km, $h_R = 5$ km, $\tau = 45°$	50 mm/h	33.825 dB	NR
Luxembourg-like: 49.6°, 0.3 km, $h_R = 5.2$ km, $\tau = 0°$	50 mm/h	30.491 dB	NR

show heavy-rain Ka-band outage across the tested grid, while profile-dependent sensitivity appears under clear-sky and 10 mm/h conditions, where BLER transitions remain within the grid.

C. Uplink BLER Sensitivity to Rain Attenuation

We repeated the PHY-level weather sweep in `nr_ulsim` using the same NTN-TDL profiles, carrier bands, elevation angles, rain-rate inputs, SNR grid, and 1000 trials per point. The UL configuration used numerology 0 with a 25 PRB carrier grid and an explicitly scheduled 25 PRB PUSCH allocation, required because `nr_ulsim`'s default PUSCH allocation exceeds a 25 PRB carrier grid.

Fig. 4 shows the UL results follow the same rain-attenuation structure as DL. For `NTN_TDL_C`, S-band is essentially unchanged, with added loss below 0.1 dB. At 14 GHz, 50 mm/h rain at 30° shifts the BLER≤ 0.1 point to 20 dB. At 20 GHz, 10 mm/h shifts the threshold to 12 dB, while 50 mm/h is not recovered within the tested -4–24 dB grid – as in the DL case, this NR entry reflects expected heavy-rain Ka-band outage.

These UL results are not meant to reveal a different rain mechanism, but to confirm that the same large-scale rain-loss abstraction behaves consistently under the uplink simulator and its explicit 25 PRB PUSCH allocation. Differences between DL and UL absolute thresholds mainly reflect simulator-side PHY and receiver-chain details, while the weather conclusion holds for both directions: S-band is rain-insensitive, Ku-band consumes meaningful link margin, and Ka-band becomes the limiting case under heavy rain. This matched DL/UL behavior confirms that rain attenuation is implemented as a direction-independent Earth-space loss term, not a direction-specific change to the small-scale fading taps.

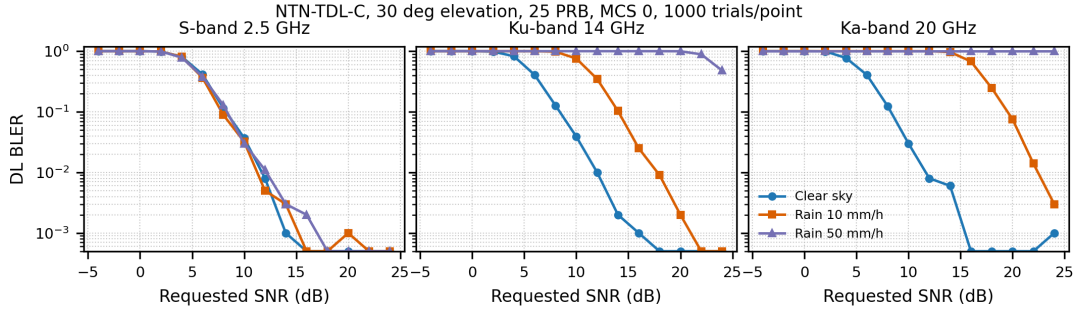


Fig. 3. Selected DL BLER rain-attenuation sensitivity for `NTN_TDL_C` at 30° elevation with 25 PRB, MCS 0, and 1000 trials per SNR point. Rain has negligible effect at S-band, shifts the Ku-band waterfall, and causes severe Ka-band degradation under 50 mm/h rain.

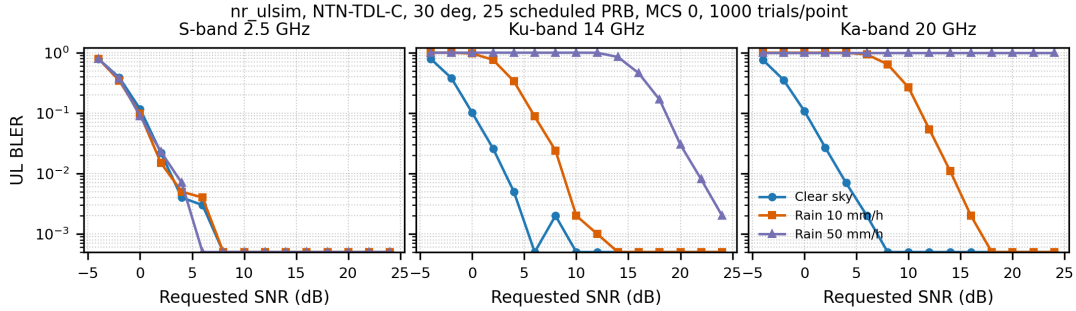


Fig. 4. Selected UL BLER rain-attenuation sensitivity for `NTN_TDL_C` at 30° elevation with numerology 0, 25 PRB carrier, 25 PRB scheduled PUSCH, MCS 0, and 1000 requested trials per SNR point. The UL sweep reproduces the same band-dependent behavior observed in DL: negligible S-band impact, Ku-band degradation, and severe Ka-band degradation under heavy rain.

TABLE VI
REQUESTED SNR FOR DL BLER ≤ 0.1 AT KA-BAND 20 GHZ (1000 TRIALS/POINT); NR MEANS NOT REACHED IN THE TESTED -4–24 DB SNR GRID

Prof.	Clear	10@30°	50@30°	50@60°
A	20 dB	NR	NR	NR
B	20 dB	NR	NR	NR
C	10 dB	20 dB	NR	NR
D	12 dB	22 dB	NR	NR

TABLE VII
REQUESTED SNR FOR UL BLER ≤ 0.1 AT KA-BAND, 20 GHZ (1000 TRIALS/POINT). NR: NOT REACHED WITHIN -4–24 DB.

Prof.	Clear	10@30°	50@30°	50@60°
A	6 dB	16 dB	NR	NR
B	6 dB	18 dB	NR	NR
C	2 dB	12 dB	NR	NR
D	2 dB	14 dB	NR	NR

D. End-to-End Attach Under Rain

To verify that the rain term is not limited to offline PHY evaluation, we also exercised the RFsim runtime path with paired OAI gNB/UE softmodems. The matrix in Table VIII uses GEO NTN-TDL-C under pinned LOS rain conditions, adds pinned NLOS moderate-rain checks, and includes additional requested-profile checks for NTN-TDL-A/B/D at 30°, including D-profile heavy-rain LOS/NLOS cases. These added runs exercise both LOS-to-LOS and NLOS-to-NLOS remapping branches while keeping the same S-band rain-loss computation. The RFsim attach configuration uses the NR NTN S-band pair from the gNB/UE configuration, with downlink at 2.486 GHz and uplink at 1.612 GHz; DL and UL rain losses are therefore expected to differ. A PASS entry denotes successful SSB synchronization, SIB1/SIB2/SIB19 decoding, random access, NAS registration accept, PDU session establishment accept, and user-plane `oaitun_ue1` creation, identified in the logs as the progression `Initial sync` → `SIB1 decoded/SIB19` → `RA procedure succeeded` → `Registration Accept` → `PDU Session Accept` → `oaitun_ue1`. We observe the following from Table VIII:

Attach and Channel Profile Remapping Outcome: All rows in Table VIII reach PASS, confirming that the rain-adjusted large-scale state is visible on the live RFsim `chanmod` path while preserving the full 5G-NTN SA control-plane and user-plane attach sequence. The 30° rows further show that requested A/B/D profiles resolve to the expected effective LOS/NLOS tap families: A→C under LOS, A→A under NLOS, B→D under LOS, B→B under NLOS, D→D under LOS, and D→B under NLOS, with the D-profile rows confirming the same behavior under heavy rain. The additional NLOS row requests `SAT_GEO_NTN_TDL_C` but resolves to effective `SAT_GEO_NTN_TDL_A`, confirming that the rain term does not bypass the existing LOS/NLOS remapping path.

TABLE VIII
FULL RFSIM 5G SA ATTACH EVIDENCE FOR GEO RAIN CASES (DL/UL RAIN LOSS AND ATTACH OUTCOME PER CONFIGURATION)

Req.	Elev.	State/Eff.	Weather	$R_{0.01}$	DL loss	UL loss	Attach
C	30°	LOS/C	clear-sky	0 mm/h	0.000000 dB	0.000000 dB	PASS
C	30°	LOS/C	moderate rain	10 mm/h	0.017091 dB	0.005253 dB	PASS
C	30°	NLOS/A	moderate rain	10 mm/h	0.017091 dB	0.005253 dB	PASS
A	30°	LOS/C	moderate rain	10 mm/h	0.017091 dB	0.005253 dB	PASS
A	30°	NLOS/A	moderate rain	10 mm/h	0.017091 dB	0.005253 dB	PASS
B	30°	LOS/D	moderate rain	10 mm/h	0.017091 dB	0.005253 dB	PASS
B	30°	NLOS/B	moderate rain	10 mm/h	0.017091 dB	0.005253 dB	PASS
D	30°	LOS/D	moderate rain	10 mm/h	0.017091 dB	0.005253 dB	PASS
D	30°	NLOS/B	moderate rain	10 mm/h	0.017091 dB	0.005253 dB	PASS
D	30°	LOS/D	heavy rain	50 mm/h	0.069278 dB	0.017740 dB	PASS
D	30°	NLOS/B	heavy rain	50 mm/h	0.069278 dB	0.017740 dB	PASS
C	30°	LOS/C	heavy rain	50 mm/h	0.069278 dB	0.017740 dB	PASS
C	60°	LOS/C	clear-sky	0 mm/h	0.000000 dB	0.000000 dB	PASS
C	60°	LOS/C	moderate rain	10 mm/h	0.009767 dB	0.002887 dB	PASS
C	60°	LOS/C	heavy rain	50 mm/h	0.035551 dB	0.008822 dB	PASS

Rain Attenuation Behavior: As expected from the P.618/P.838 calculation, rain loss is larger at 30° than at 60° due to the longer effective Earth-space rain path, and DL loss exceeds UL loss throughout because the downlink carrier (2.486 GHz) is higher than the uplink carrier (1.612 GHz).

Scope: This test is intentionally an attach sanity check rather than a throughput benchmark. Throughput characterization under controlled, real-time-capable execution conditions is planned as a complementary evaluation; the present attach-focused validation establishes that the rain-adjusted channel state is correctly applied end to end.

V. CONCLUSION AND FUTURE WORK

This paper presented an ITU-R rain-attenuation extension for a GEO NTN-TDL channel emulator in OAI RFsim. A compact TR 38.811-based GEO NTN-TDL substrate provides the small-scale tap profiles, LOS/NLOS remapping, and large-scale GEO state on which the rain term is applied, using ITU-R P.618 $A_{0.01}$ rain attenuation derived from P.838 coefficients and exposing $R_{0.01}$, frequency, elevation, rain height, station altitude, latitude, and polarization tilt as configurable inputs. Sanity checks confirm the expected zero-rain, rain-rate, elevation, and band-dependent attenuation behavior; 1000-trial DL and UL PHY sweeps show rain impact is negligible at S-band, material at Ku-band, and can drive Ka-band links into outage under heavy rain. Selected full RFsim gNB/UE runs for GEO NTN-TDL-C LOS/NLOS rain cases, together with additional A/B/D profile checks, further confirm that clear-sky, moderate-rain, and heavy-rain configurations preserve complete 5G SA attach at the tested S-band settings. The result is a reproducible OAI-based framework for studying rain sensitivity on top of TR 38.811-aligned GEO NTN channel conditions.

Ongoing work includes deriving $R_{0.01}$ from ITU-R P.837/P.839 climatic maps; slant-range-derived GEO propagation delay in place of the current SIB19-aligned `prop_delay`; additional atmospheric terms including gases, clouds, and scintillation, with time-percentage extrapolation beyond $A_{0.01}$; dynamic LOS/NLOS remapping; time-varying weather traces; and broader RFsim rain campaigns including throughput measurements. The implementation and validation artifacts are being prepared for upstream submission to OAI's `develop` branch.

ACKNOWLEDGMENT

This work was supported by WEBSAT-6G through 6G-PATH Open Call 2 (SNS JU Horizon Europe, Grant Agreement No. 101139172).

REFERENCES

[1] 3GPP, "Study on New Radio (NR) to support non-terrestrial networks," 3rd Generation Partnership Project (3GPP), Technical Report (TR) 38.811, Oct. 2019, release 15. [Online]. Available: https://portal.3gpp.org/desktopmodules/Specifications/SpecificationDetails.aspx?specificationId=3234

[2] ITU-R, "Propagation data and prediction methods required for the design of Earth-space telecommunication systems," International Telecommunication Union, Recommendation ITU-R P.618-14, Aug. 2023. [Online]. Available: https://www.itu.int/rec/R-REC-P.618-14-202308-I/en

[3] ——, "Specific attenuation model for rain for use in prediction methods," International Telecommunication Union, Recommendation ITU-R P.838-3, Mar. 2005. [Online]. Available: https://www.itu.int/rec/R-REC-P.838-3-200503-I/en

[4] OpenAirInterface Software Alliance, "OpenAirInterface5G: OpenAir-Interface 5G Wireless Implementation," 2015, gitLab repository, Apache License 2.0. Accessed: 2026-06-10. [Online]. Available: https://gitlab.eurecom.fr/oai/openairinterface5g

[5] MathWorks, "Model NR NTN Channel," Satellite Communications Toolbox documentation, 2024, accessed Jun. 2026. [Online]. Available: https://nl.mathworks.com/help/satcom/ug/model-nr-ntn-channel.html

[6] T. Düe, M. Vakilifard, C. Bockelmann, D. Wübben, and A. Dekorsy, "An open source channel emulator for non-terrestrial networks," in *Advanced Satellite Multimedia Systems Conference/Signal Processing for Space Communications Workshop (ASMS/SPSC 2025)*, 2025.

[7] M. Sandri, M. Pagin, M. Giordani, and M. Zorzi, "Implementation of a channel model for non-terrestrial networks in ns-3," in *Proc. Workshop on ns-3 (WNS3)*, Arlington, VA, USA, Jun. 2023, arXiv:2305.05544.

[8] Magister Solutions, "SNS3: Satellite network simulator 3," 2024, ns-3 satellite extension module developed under ESA contract. Accessed: 2026-06-11. [Online]. Available: https://github.com/sns3/sns3-satellite

[9] Software Radio Systems, "srsRAN Project: Open-source O-RAN 5G RAN," 2023, gitLab/GitHub repository. Accessed: 2026-06-11. [Online]. Available: https://github.com/srsran/srsRAN_Project

[10] ——, "srsRAN gNB for 5G NTN," srsRAN Project documentation, 2024, accessed: 2026-06-11. [Online]. Available: https://docs.srsran.com/projects/project/en/latest/tutorials/source/ntn/source/index.html

[11] S. Kumar, A. K. Meshram, A. Astro, J. Querol, S. Chatzinotas, T. Schlichter, G. Casati, T. Heyn, F. Völk, S. Kaya, R. T. Schwarz, A. Knopp, P. Marques, L. Pereira, R. Magueta, A. Kapovits, and F. Kaltenberger, "OpenAirInterface as a platform for 5G-NTN research and experimentation," in *Proc. IEEE Future Netw. World Forum (FNWF)*, 2022, pp. 500–506.

[12] S. Kumar, A. Astro, O. Kodheli, J. Querol, S. Chatzinotas, T. Schlichter, G. Casati, T. Heyn, F. Völk, S. Kaya, R. T. Schwarz, A. Knopp, A. Kapovits, and F. Kaltenberger, "5G-NTN GEO-based in-lab demonstrator using OpenAirInterface5G," in *Proc. 11th Adv. Satellite Multimedia Syst. Conf. (ASMS)*, 2022.

[13] S. Kumar, O. Kodheli, A. Astro, J. Querol, S. Chatzinotas, G. Casati, T. Schlichter, T. Heyn, H. Cheporniuk, F. Völk, R. T. Schwarz, A. Knopp, A. Kapovits, and F. Kaltenberger, "5G-NTN GEO-based over-the-air demonstrator using OpenAirInterface," in *Proc. 39th Int. Commun. Satellite Syst. Conf. (ICSSC)*, 2022.

[14] F. Völk, T. Schlichter, S. Kumar, R. T. Schwarz, A. Knopp, M. Hammouda, T. Heyn, J. Querol, S. Chatzinotas, and A. Kapovits, "5G Non-Terrestrial Networks With OpenAirInterface: An experimental study over GEO satellites," *IEEE Access*, vol. 12, pp. 155 098–155 109, 2024.

[15] S. Kumar, C. K. Sheemar, J. Querol, T. Yilmaz, S. Chatzinotas, M. Hammouda, O. Kodheli, A. Astro, and F. Kaltenberger, "5G NTN LEO based demonstrator using OpenAirInterface5G," in *IET Conf. Proc.*, vol. 2023, no. 48, 2023, pp. 69–75.